Multimodal evaluation of a porous HA/β-TCP scaffold for bone repair and localized therapy in rats

Dr. Ashok R. Unni
Assistant Professor, Department of Veterinary Medicine, **Amrita Hospital**, An Institute of Amrita Vishwa Vidyapeetham, Kerala, India

INTRODUCTION

- Bone is a dynamic, load-bearing connective tissue for support, protection, locomotion, haematopoiesis & mineral storage
- Fracture disrupts continuity; a critical-size defect (CSD ≥ 2.5 × diaphyseal diameter) fails spontaneous repair; demands graft
- Morbidity, supply limits and disease/rejection risks limit the use of autografts and allografts
- Synthetic ceramics mimic bone mineral and support bonding, while a porous structure enables drug loading

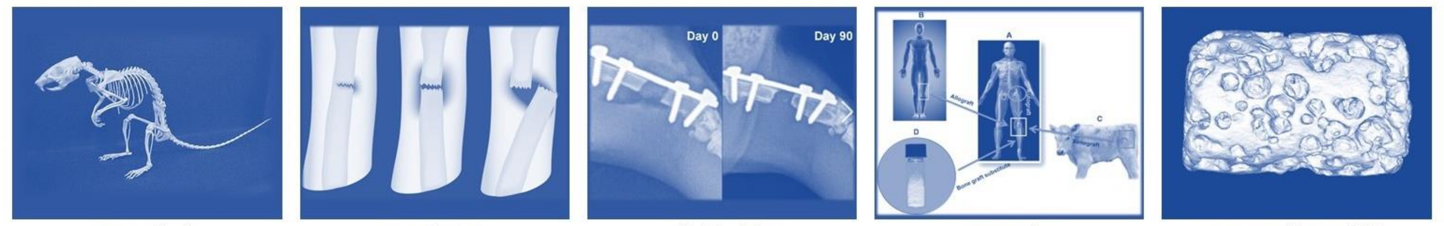

Bones of body | Bone fracture | Critical size defect | Bone grafts | Porous HA/β-TCP scaffold

- Hydroxyapatite (HA) offers high osteoconductivity, high mechanical strength but low biodegradation
- β-Tricalcium phosphate (β-TCP) offers rapid resorption, chemotaxis but reduced mechanical strength
- A porous biphasic HA/β-TCP scaffold can offer synergistic osteoconduction, controlled degradation, chemotaxis, and mechanical strength, while also serving as a biodegradable reservoir for controlled local drug delivery
- The present study provides an *in vivo* multimodal evaluation in a rat femoral CSD model

MATERIALS & METHODS

- Biphasic calcium phosphate scaffold composed of β-tricalcium phosphate (40%) and hydroxyapatite (60%)
- 60% interconnected porosity distributed across macro, meso and micro levels
- Mechanical strength intermediate between porous HA and βTCP; resorbs faster than pure HA
- Fabricated using an indigenously developed gel-casting technique, followed by drying and sintering
- Characterized for chemical purity, crystallinity, morphology, mechanical strength and porosity
- Preliminary *in vitro* studies confirmed biological suitability
- Scaffolds sized as 3 mm diameter × 7.5 mm length cylinders for implantation

80 Healthy male Wistar rats, 08 weeks Old, 200g bodyweight | Rats were evaluated 12 hours pre-anesthesia and fasted for 3 hours before anesthesia induction | Rats were sedated (IM xylazine, tramadol) and anaesthetized (IP ketamine, midazolam) | The right thigh was shaved and aseptically prepared with chlorhexidine and povidone-iodine | Micro Surgery Instrument Set

Plating Surgery Instrument Set | A skin incision over the thigh exposed the muscles by separating subcutaneous tissue and fascia | Femur was exposed by dissection and muscle retraction; site was cleaned with metronidazole | A 1.5 mm 4-holed stainless-steel plate was secured to the femur with nylon at three points | Four pilot holes were drilled and widened on the lateral cortex under saline irrigation

A 1.5 mm × 5 mm screw was placed proximally and the nylon ties were removed | The plate was rotated caudally on the proximal screw hinge; site was cleaned with metronidazole | A 7.5 mm femoral defect was created, bone removed, and cut ends smoothened | The plate was rotated cranially onto the femur using the proximal screw hinge | The plate and bone fragments were aligned and fixed with 1.5 mm × 5 mm screws

A 7.5 × 3 mm HA-βTCP scaffold was placed in the bone defect | The scaffold was secured in place with nylon sutures; nylon muscle retractions were removed | Muscles and fascia were closed with nylon in a simple continuous pattern | Skin closed with nylon in a simple continuous pattern; site disinfected with povidone-iodine | Rats received antibiotics, analgesics, and wound spray for 1-week post-surgery

- This study employed multimodal evaluation, integrating radiography, 7T magnetic resonance imaging, micro-computed tomography, biomechanical testing and histopathology to assess bone healing and scaffold performance.
- The study was conducted following the guidelines of the Institutional Animal Ethics Committee (IAEC) and overseen by the Committee for the Control and Supervision of Experiments on Animals (CCSEA).

RESULTS & DISCUSSION

- Radiograph: Right Femur, Oblique Medio Lateral view, Scale 5mm

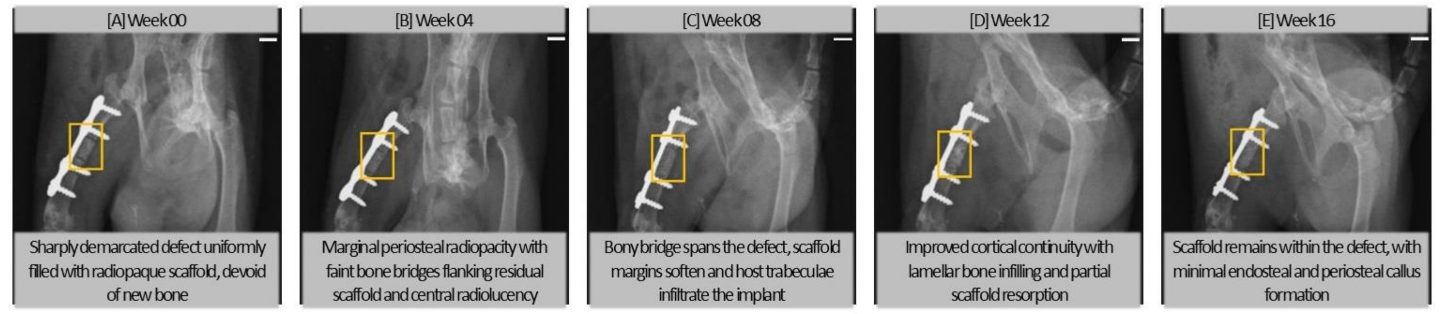

[A] Week00: Sharply demarcated defect uniformly filled with radiopaque scaffold, devoid of new bone | [B] Week04: Marginal periosteal radiopacity with faint bone bridges flanking residual scaffold and central radiolucency | [C] Week08: Bony bridge spans the defect, scaffold margins soften and host trabeculae infiltrate the implant | [D] Week12: Improved cortical continuity with lamellar bone infilling and partial scaffold resorption | [E] Week16: Scaffold remains within the defect, with minimal endosteal and periosteal callus formation

- 7T Magnetic Resonance Imaging: Right Femur, Coronal plane, Scale 5mm

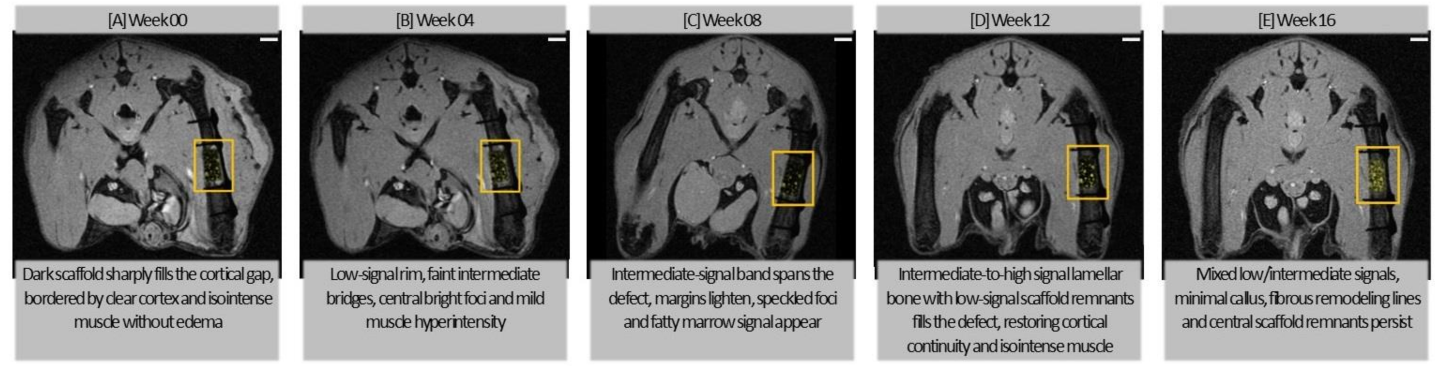

[A] Week00: Dark scaffold sharply fills the cortical gap, bordered by clear cortex and isointense muscle without edema | [B] Week04: Low-signal rim, faint intermediate bridges, central bright foci and mild muscle hyperintensity | [C] Week08: Intermediate-signal band spans the defect, margins lighten, speckled foci and fatty marrow signal appear | [D] Week12: Intermediate-to-high signal lamellar bone with low-signal scaffold remnants fills the defect, restoring cortical continuity and isointense muscle | [E] Week16: Mixed low/intermediate signals, minimal callus, fibrous remodeling lines and central scaffold remnants persist

- 7T Magnetic Resonance Imaging: Right Femur, Axial plane, Scale 5mm

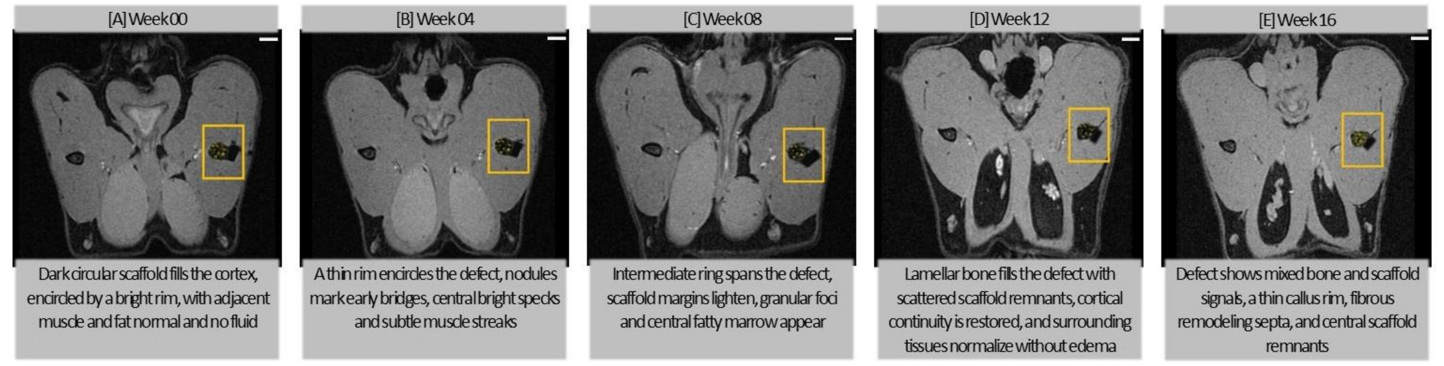

[A] Week00: Dark circular scaffold fills the cortex, encircled by a bright rim, with adjacent muscle and fat normal and no fluid | [B] Week04: A thin rim encircles the defect, nodules mark early bridges, central bright specks and subtle muscle streaks | [C] Week08: Intermediate ring spans the defect, scaffold margins lighten, granular foci and central fatty marrow appear | [D] Week12: Lamellar bone fills the defect with scattered scaffold remnants, cortical continuity is restored, and surrounding tissues normalize without edema | [E] Week16: Defect shows mixed bone and scaffold signals, a thin callus rim, fibrous remodeling septa, and central scaffold remnants

- 7T Magnetic Resonance Imaging: Right Femur, Sagittal plane, Scale 5mm

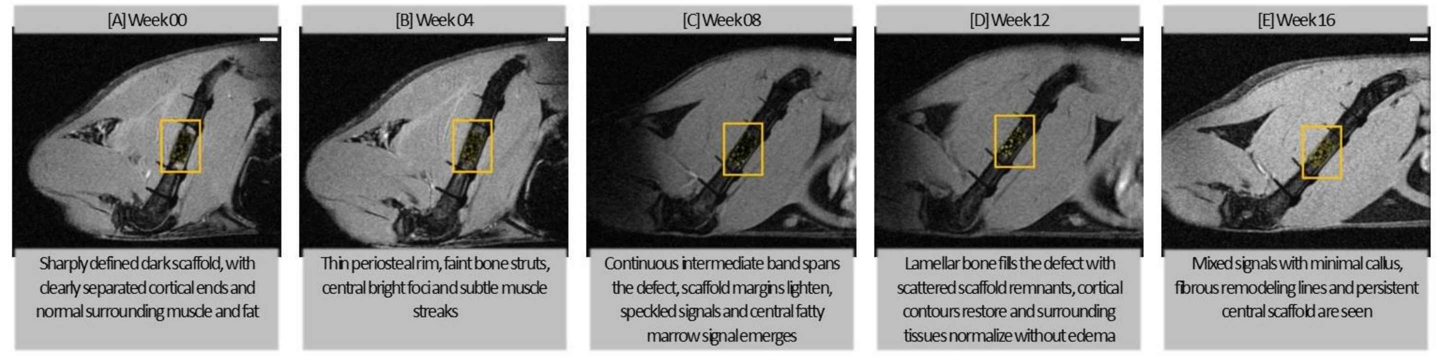

[A] Week00: Sharply defined dark scaffold, with clearly separated cortical ends and normal surrounding muscle and fat | [B] Week04: Thin periosteal rim, faint bone struts, central bright foci and subtle muscle streaks | [C] Week08: Continuous intermediate band spans the defect, scaffold margins lighten, speckled signals and central fatty marrow signal emerges | [D] Week12: Lamellar bone fills the defect with scattered scaffold remnants, cortical contours restore and surrounding tissues normalize without edema | [E] Week16: Mixed signals with minimal callus, fibrous remodeling lines and persistent central scaffold are seen

- Computed Tomography: Left Femur, Two-Dimensional, Growing Cortex

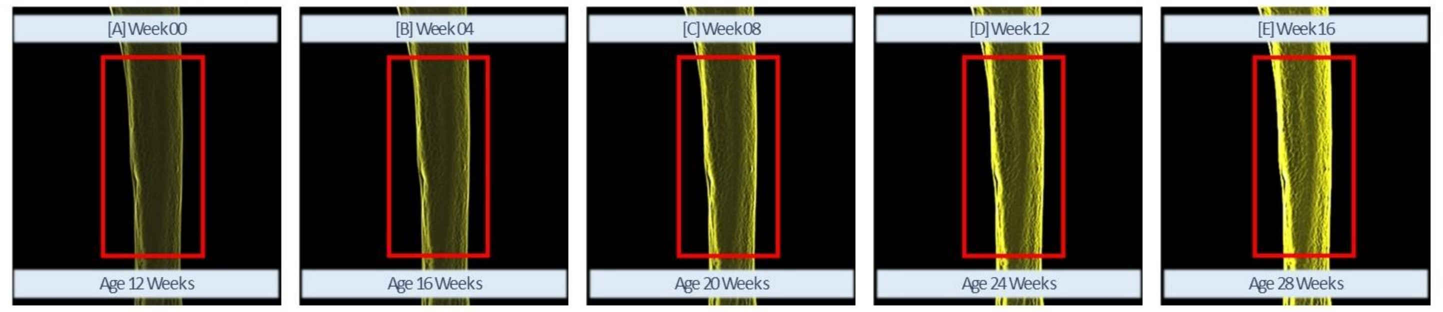

[A] Week00 – Age 12 Weeks | [B] Week04 – Age 16 Weeks | [C] Week08 – Age 20 Weeks | [D] Week12 – Age 24 Weeks | [E] Week16 – Age 28 Weeks

- Computed Tomography: Right Femur, Three-Dimensional Reconstruction, Scaffold Degradation

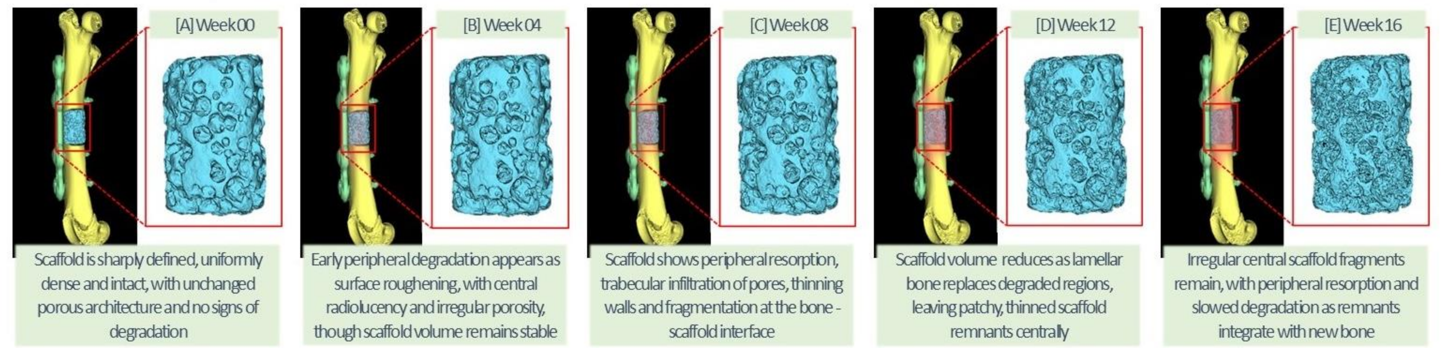

[A] Week00: Scaffold is sharply defined, uniformly dense and intact, with unchanged porous architecture and no signs of degradation | [B] Week04: Early peripheral degradation appears as surface roughening, with central radiolucency and irregular porosity, though scaffold volume remains stable | [C] Week08: Scaffold shows peripheral resorption, trabecular infiltration of pores, thinning walls and fragmentation at the bone - scaffold interface | [D] Week12: Scaffold volume reduces as lamellar bone replaces degraded regions, leaving patchy, thinned scaffold remnants centrally | [E] Week16: Irregular central scaffold fragments remain, with peripheral resorption and slowed degradation as remnants integrate with new bone

- Computed Tomography: Right Femur, Three-Dimensional Reconstruction, Cellular Infiltration

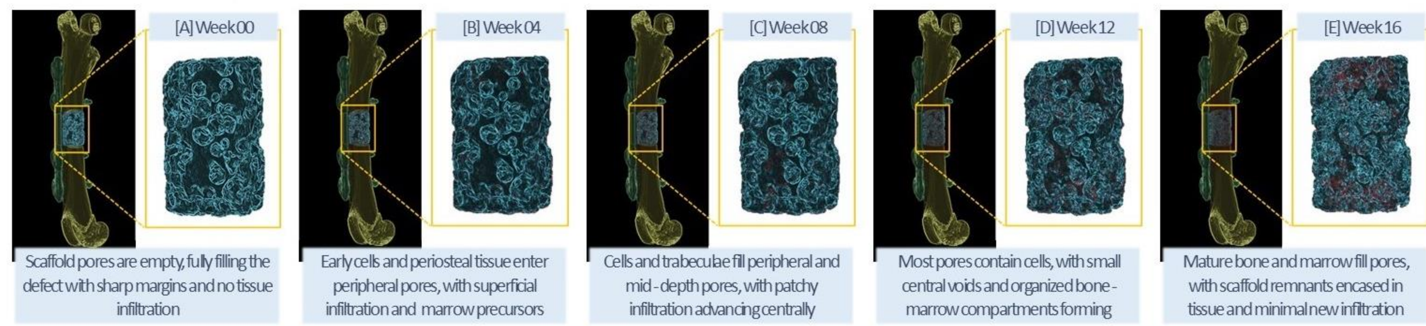

[A] Week00: Scaffold pores are empty, fully filling the defect with sharp margins and no tissue infiltration | [B] Week04: Early cells and periosteal tissue enter peripheral pores, with superficial infiltration and marrow precursors | [C] Week08: Cells and trabeculae fill peripheral and mid - depth pores, with patchy infiltration advancing centrally | [D] Week12: Most pores contain cells, with small central voids and organized bone - marrow compartments forming | [E] Week16: Mature bone and marrow fill pores, with scaffold remnants encased in tissue and minimal new infiltration

- Computed Tomography: ROI [Bone/Biomaterial/New Bone] Volume Evaluation [mm3]

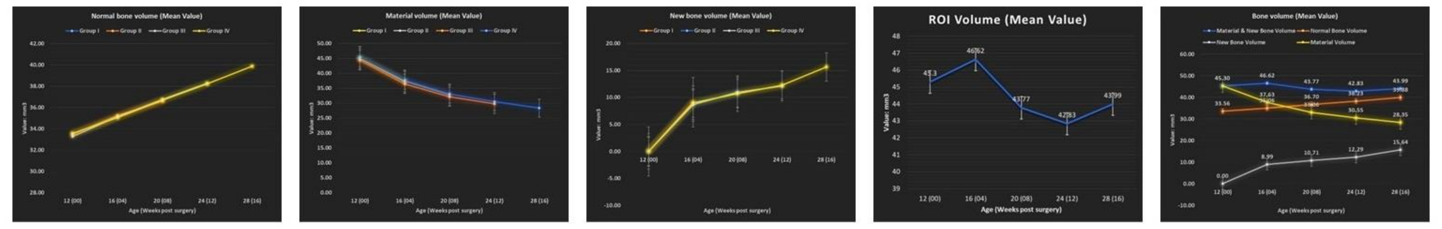

- Computed Tomography: ROI [Bone/Biomaterial/New Bone] Density Evaluation [mg/mm3]

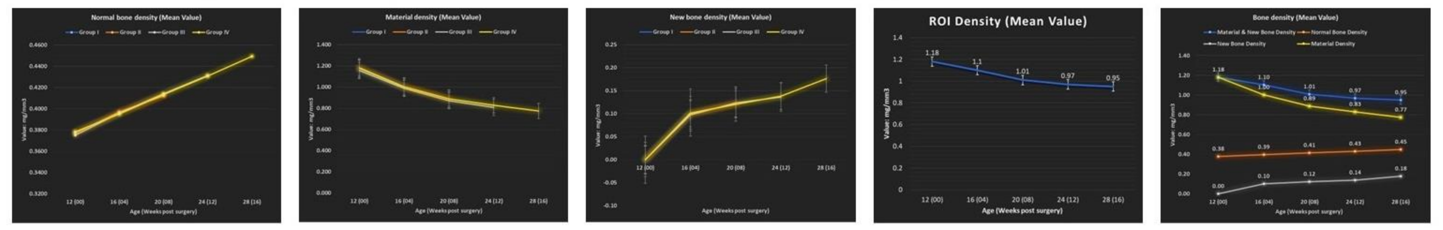

- Biomechanical Testing: Normal and Healing Femur [Bending test, Torsion test and Compression test]

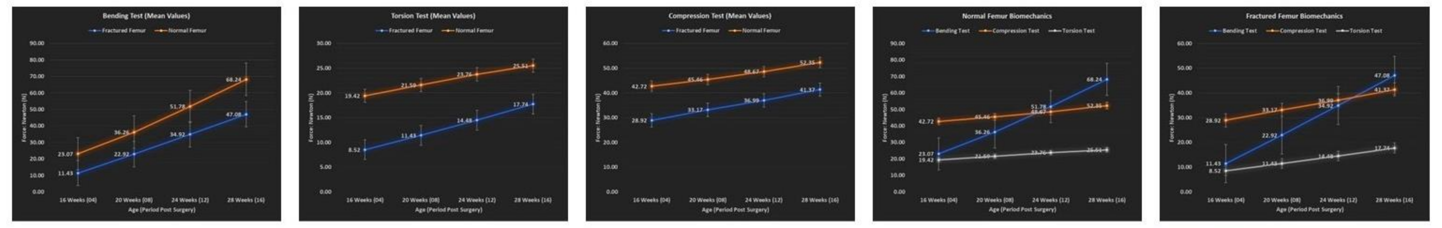

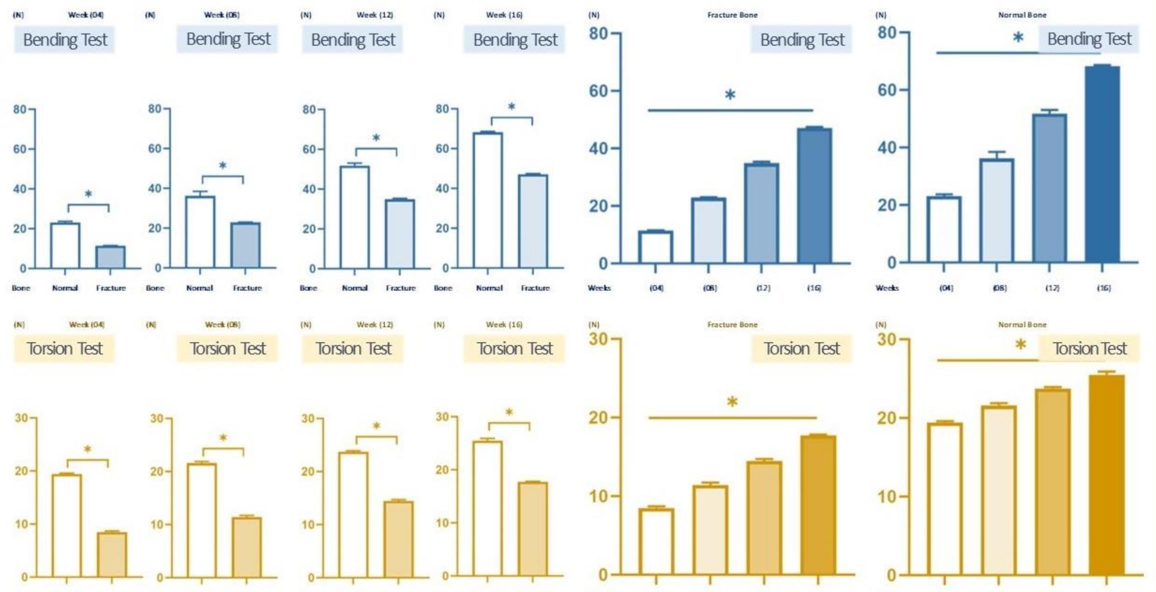

Normal Femur: Maintained high mechanical strength with intact cortical and trabecular structure, showing no weakness or degradation

Untreated CSD: No measurable biomechanical strength, no tissue

Week 0: No measurable biomechanical strength; defect stabilized solely by the scaffold's passive structure without tissue contribution

Week 04: Minimal mechanical recovery observed; scaffold and early fibrous bridging provided limited load-bearing capacity, well below intact bone levels

Week 08: Progressive strength restoration across bending, torsion, and compression; early bone bridging and scaffold resorption improved mechanical integrity

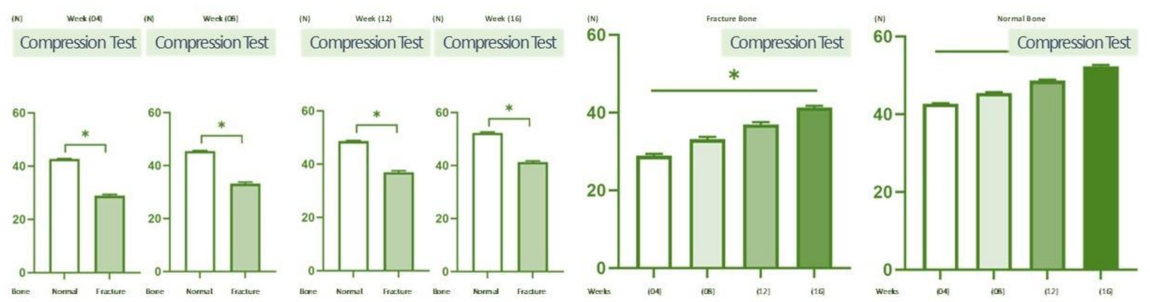

Week 12: Significant biomechanical gains as cortical continuity and lamellar bone formation advanced; scaffold degradation facilitated functional recovery, though strength remained inferior to intact bone

Week 16: Mechanical properties approached functional stability; immature bone and residual scaffold fragments supported the defect, but complete biomechanical restoration was not achieved

- Gross Specimen: Left Femur [Healing Fracture]

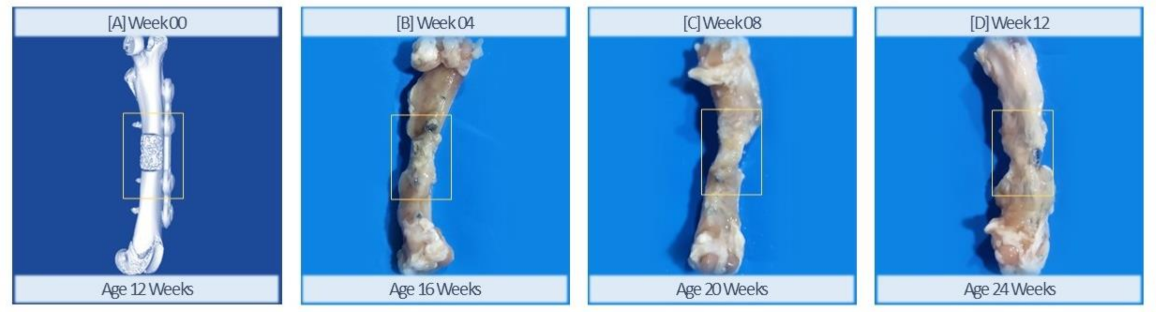

[A] Week00 – Age 12 Weeks | [B] Week04 – Age 16 Weeks | [C] Week08 – Age 20 Weeks | [D] Week12 – Age 24 Weeks | [E] Week16 – Age 28 Weeks

- Histopathology: [Hematoxylin & Eosin Stain, Masson's Trichrome Stain and Van Gieson's Stain]

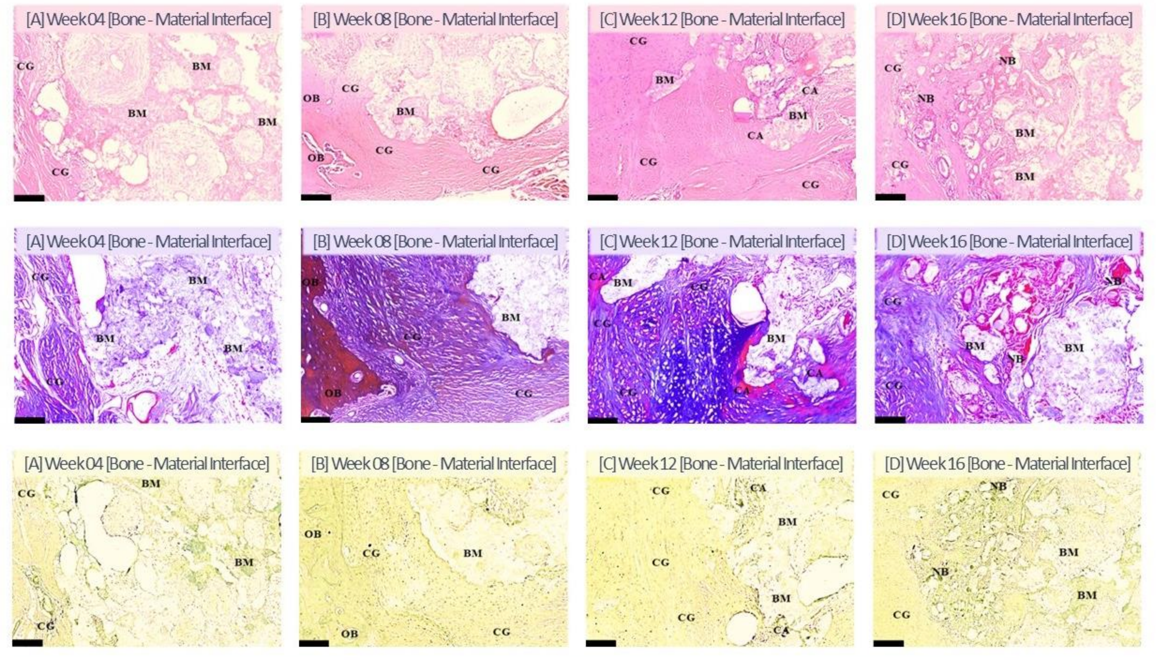

Magnification 100X; Scale Bar: 200µm; BM: Biomaterial; CG: Collagen; CA: Cartilage; NB: New bone; OB: Old bone

Normal Femur: Thick lamellar cortex, dense trabeculae, healthy marrow, and no fibrosis or defects

Week 04: The scaffold remained well-positioned and intact, encased by a thin fibrous tissue bridge without evidence of degradation or cellular ingrowth

Week 08: The defect was bridged by a dense fibrous matrix enveloping the scaffold, with early βTCP resorption at the scaffold margins. Fibrous tissue and chondroblast-like cells infiltrated the peripheral pores

Week 12: The defect space was largely filled with fibrous-cartilaginous tissue, and scaffold pores showed sparse transformation into cartilage. βTCP degradation advanced, leaving isolated HA fragments

Week 16: The scaffold remained aligned within the defect, surrounded by fibrocartilage and immature woven bone. βTCP was mostly resorbed, while HA persisted. Scaffold pores contained early bone tissue.

CONCLUSIONS

- Porous hydroxyapatite/β-tricalcium phosphate (HA/βTCP) scaffolds enabled bone regeneration in critical-sized femoral defects, which do not heal spontaneously.
- Multimodal imaging (X-ray, 7T MRI, micro-CT) confirmed progressive scaffold degradation, defect bridging, and minimal periosteal and endosteal callus formation.
- Histopathology demonstrated endochondral ossification, with fibrous tissue gradually replaced by immature bone.
- Biomechanical testing showed significant strength recovery compared to untreated defects, although below that of intact bone.
- The scaffold provided early structural support and guided cellular infiltration and tissue remodelling.
- Its porous structure facilitates localized delivery of cells, growth factors, and therapeutic agents.
- HA/βTCP scaffolds represent a promising alternative to autografts for large bone defects and a potential drug delivery platform.
- Further refinement is needed to achieve complete mechanical and functional restoration.

References

- Costa, C.M., Bernardes, G., Ely, J.B. and Porto, L.M., 2011. Proposal for access to the femur in rats. International Journal of Biotechnology and Molecular Biology Research, 2(4), pp.73-79.
- Sureshbabu, S., Komath, M. and Varma, H.K., 2012. In situ formation of hydroxyapatite–αlpha tricalcium phosphate biphasic ceramics with higher strength and bioactivity. Journal of the American Ceramic Society, 95(3), pp.915-924.
- Gallinetti, S., Canal, C., Ginebra, M. P. and Ferreira, J. 2014. Development and Characterization of Biphasic Hydroxyapatite/β-TCP Cements. J. Am. Ceram. Soc. 97(4): 1065-1073.
- Unni, A.R., Syam, K.V., John, M.K.D., Anoop, S., Maya, S. and Dhanush, K.B., 2024. Biomechanical evaluation of healing of critical-sized long bone defects in rats treated with biphasic hydroxyapatite (HA) and β-tricalcium phosphate (β-TCP) bioceramic scaffolds. J. Vet. Anim. Sci, 55(3), pp.580-585.
- Ashok, R.U., Syam, K.V., John Martin, K.D., Anoop, S., Maya, S. and Dhanush Krishna, B., 2024. Serum biochemical evaluation of healing of critical-sized long bone defects in rats treated with biphasic hydroxyapatite (HA) and β-tricalcium phosphate (β-TCP) bioceramic scaffolds. J. Vet. Anim. Sci, 55(3), pp.586-592.